

# Folding Dynamics of Ferrocyanochrome *c* in a Denaturant-Free Environment Probed by Transient Grating Spectroscopy

Jungkweon Choi,<sup>[a]</sup> Yang Ouk Jung,<sup>[a]</sup> Jae Hyuk Lee,<sup>[a]</sup> Cheolhee Yang,<sup>[a]</sup> Bongsoo Kim,<sup>\*,[b]</sup> and Hyotcherl Ihee<sup>\*,[a]</sup>

There have been numerous experimental and theoretical studies that aim to clarify the folding process occurring in biological systems, but many unsolved important questions still remain for protein folding.<sup>[1–8]</sup> Generally, the folding processes of most proteins have been interpreted by two-state or sequential mechanisms.<sup>[2,5,9–11]</sup> The two-state mechanism involves a transition from the unfolded state to the folded state without any detectable intermediates, whereas the sequential mechanism comprises multistate transitions through intermediates. To illuminate the detailed mechanism of protein folding processes, it is important to detect and characterize the species and intermediates involved in the folding process. Folding intermediates are short-lived, often heterogeneous, and cannot be studied by the usual crystallographic or NMR methods. Therefore, faster spectroscopic methods, such as time-resolved infrared,<sup>[12]</sup> time-resolved circular dichroism (CD),<sup>[5,6,13,14]</sup> transient absorption,<sup>[15]</sup> and stopped-flow optical spectroscopic methods,<sup>[3,16]</sup> have been utilized. These diverse methods can provide reaction rates, signal the accumulation of intermediates, and give local information on the role of particular amino acids or averaged parameters of the main chain. However, they do not provide global structural information in general.

In this respect, the diffusion coefficient ( $D$ ), which represents molecular migration in the liquid phase, is certainly a useful quantity for monitoring a protein-folding process because it is a fundamental physical parameter directly linked to the macromolecular size and shape. Indeed, Terazima and co-workers have shown that the change in diffusion coefficient reflects the conformational change of a biomolecule that occurs in the process of various biological reactions, such as protein folding.<sup>[17–20]</sup> They used laser-induced transient grating (TG) spectroscopy to measure the change in  $D$  followed by a protein folding process.<sup>[17–20]</sup> The TG technique can detect a spatial concentration modulation of chemical species induced by laser irradiation. From the temporal profile of the TG signal intensity, the  $D$  values of the parent molecule and transient species involved in a photoreaction can be determined directly from the decay rate of the signal measured. In summary, TG spectroscopy

provides information about global structural change, whereas transient absorption is more sensitive to local structure and CD is informative for secondary structures.

In the study reported herein, we investigate the optically triggered folding dynamics of CO-bound ferrocyanochrome *c* (CytC-CO) under highly basic conditions (pH 13) by using time-resolved TG spectroscopy. The folding dynamics of CytC with a denaturant has been previously studied by using a combination of the electron transfer of nicotinamide adenine dinucleotide (NADH) and TG spectroscopy.<sup>[18]</sup> Our study differs in that no denaturant is used so that the effect of the denaturant can be estimated, and the photodissociation of CO is a much faster reaction-triggering method than electron transfer of NADH ( $\approx \mu\text{s}$ ),<sup>[18]</sup> thereby greatly improving the time resolution. Indeed, we captured a process of about 700 ns, which cannot be studied by the latter reaction-triggering method. CytC-CO molecules in strongly basic solution are unfolded without a denaturant, such as guanidine hydrochloride (Gd-HCl) and urea.<sup>[21]</sup> By contrast, CytC in the absence of the CO ligand has a nativelike structure in terms of secondary and tertiary structural content in strongly basic solutions (see Figure 1). There-

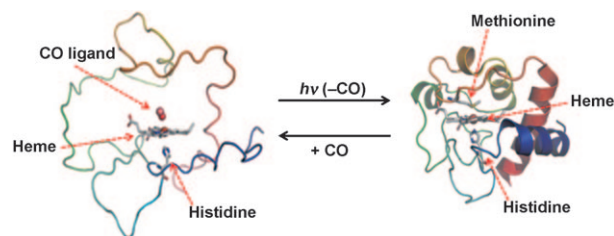


**Figure 1.** Schematic representation of the transition between folded and unfolded CytC at pH 13 considered in this work. Unlike typical folding experiments, a denaturant, such as Gd-HCl or urea, is not used, but CO ligands are used to generate CytC-CO. CytC-CO in a strong alkali solution is unfolded without a denaturant. However, CytC in the absence of CO ligand has a nativelike structure in terms of secondary and tertiary structural content in strong alkali solutions.

fore, the CO photodissociation of unfolded CytC-CO in strongly basic solution initiates folding, and CytC represents an ideal protein for studying the folding kinetics in the absence of a denaturant, thus mimicking a more natural environment for folding.

Generally, a denaturant can significantly influence the protein conformation. For example, Zhang et al. reported that the structure of the unfolded SH3 domain of *Drosophila* characterized in aqueous buffer was not identical to that characterized in 2 M Gd-HCl.<sup>[22]</sup> Furthermore, Logan et al. reported that the secondary structures of the unfolded FK506 binding protein

[a] Dr. J. Choi, Y. O. Jung, J. H. Lee, C. Yang, Prof. H. Ihee  
Center for Time-Resolved Diffraction  
Department of Chemistry, KAIST  
Daejeon 305-701 (Republic of Korea)  
Fax: (+82)42-350-2810  
E-mail: hyotcherl.ihee@kaist.ac.kr

[b] Prof. B. Kim  
Department of Chemistry (BK21), KAIST  
Daejeon 305-701 (Republic of Korea)  
Fax: (+82)42-350-2810  
E-mail: nanobio@kaist.ac.kr

determined in the presence of Gd-HCl and urea were different.<sup>[23]</sup> In addition, we can trace fast events in the folding reaction of CytC because the photodissociation of the CO ligand takes place on the sub-picosecond timescale. In this study, we observed TG signals due to the folding dynamics, and a detailed analysis shows that the folding kinetics is more consistent with the two-state mechanism than the sequential mechanism. The experimentally determined  $D$  values of both the unfolded and folded CytC at pH 13 without a denaturant provide information in terms of molecular size. The activation energy for the folding process is also determined from temperature-dependent TG signals. Together with TG spectroscopy, transient absorption (TA) spectroscopy is also used and the results show that the two methods are indispensable complements for understanding the overall protein dynamics.

Figure 2a shows TG signals for the CytC-CO sample after the photodissociation of the CO ligand in an *N*-cyclohexyl-3-amino-

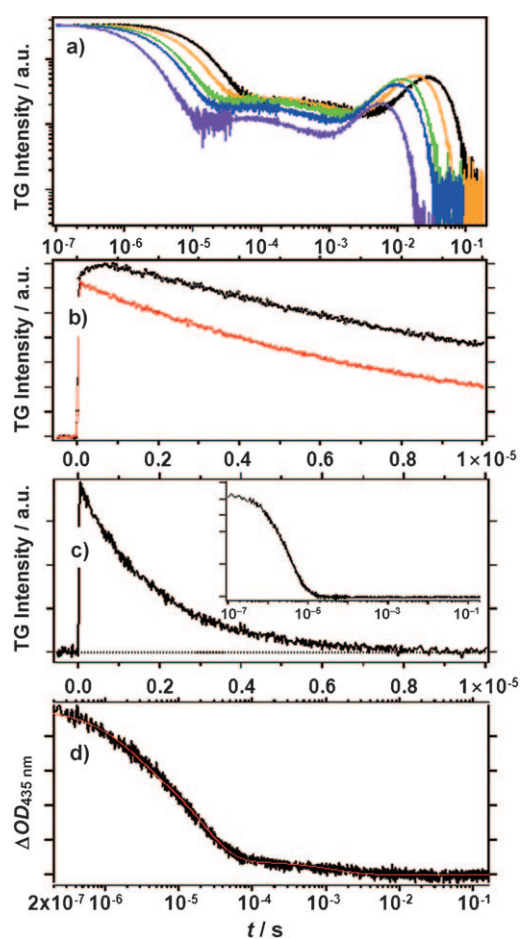


**Figure 2.** a) Time profiles of the TG signals (in log scale) after photoexcitation of CytC-CO in a CAPS buffer solution (pH 13) at various  $q^2$  ranges (from left to right,  $q^2 = 0.39, 0.62, 1.07, 1.32,$  and  $2.46 \times 10^{12} \text{ m}^{-2}$ ). b) Early-time part of the TG signals of CytC (black line) and a reference sample (bromocresol purple, red line) observed at  $q^2 = 0.39 \times 10^{12} \text{ m}^{-2}$ . c) TG signal after photoexcitation of CytC-CO under neutral conditions (pH 7) without a denaturant at  $q^2 = 1.79 \times 10^{12} \text{ m}^{-2}$ . Inset: TG signal after photoexcitation of CytC-CO at pH 7 in the presence of 6 M Gd-HCl at  $q^2 = 0.92 \times 10^{12} \text{ m}^{-2}$ . d) Transient absorption change following photolysis of 200  $\mu\text{M}$  CytC-CO in a CAPS buffer solution (pH 13). The temporal profile of the absorbance change was expressed by a triexponential function with relaxation times of  $\approx 0.9, \approx 11,$  and  $\approx 770 \mu\text{s}$ .

propanesulfonic acid (CAPS) buffer solution (pH 13) at various  $q^2$  ranges ( $q$ : grating wavenumber). All signals consist of several components. The signal rises quickly after photoexcitation within the instrumental response of our system and then shows a weak, slowly rising component (component 1), which can be seen in a temporally expanded view (the black curve in Figure 2b). After this, the signal shows a decay component in the microsecond timescale (component 2), then weak grow-decay dynamics from about 10  $\mu\text{s}$  to about 1 ms (component 3), and finally another slower grow-decay dynamics in the millisecond time range (component 4). In the following, we first qualitatively demonstrate that the observed TG signals are related to protein folding by various control experiments. Then, a more quantitative analysis is given.

As a first control experiment, a TG signal was measured from a reference sample, namely, bromocresol purple (the red curve in Figure 2b). The photon energy absorbed by bromocresol purple is nonradiatively released to the solvent without invoking any other photoreactions, and thus its TG signal reflects the thermal releasing process. The TG signal in the red curve of Figure 2b shows only a single decay component, which is similar to component 2 from the CytC sample, thus indicating that component 2 is probably the result of a thermal releasing process. The components 1, 3, and 4 are observed only for the CytC-CO sample at pH 13. To further check whether these components are related to folding dynamics, we performed another control experiment for a CytC sample under neutral conditions (pH 7), where CytC is in a folded form and therefore the energy absorbed by the heme group is released as heat to the solvent, just as the reference bromocresol purple. Indeed, the TG signal at pH 7 shown in Figure 2c has only a decay component similar to component 2 for the CytC-CO sample at pH 13, which confirms that the other components at pH 13 shown in Figure 2a may be due to the folding process.

As a further control to gauge the contribution of the bimolecular recombination of CO and CytC to the TG signal, we measured the TG signal at pH 7 in the presence of 6 M Gd-HCl where the denaturant fully converts CytC to unfolded CytC-CO, which is susceptible to photodissociation of the CO. The photoreaction of CytC-CO in this condition (pH 7) does not initiate any folding process and the bimolecular recombination process of CO and CytC should dominate.<sup>[15,21]</sup> Its TG signal in the inset of Figure 2c shows only the thermal decay, as in the signal without denaturant at pH 7, which indicates that the TG signal is not sensitive to the CO recombination process (Figure 2c). However, this does not mean that the CO recombination process is absent under our conditions. Bhuyan and co-workers<sup>[21]</sup> used TA spectroscopy to follow the dynamics of CytC-CO at pH 13 with a very low concentration of denaturant, which is similar to our denaturant-free conditions, and observed time-dependent absorption changes attributed to residue-coordination processes and the CO recombination process.

We also conducted a TA experiment as shown in Figure 2d. The TA signal can be expressed by a triexponential function with relaxation times of  $\approx 0.9, \approx 11,$  and  $\approx 770 \mu\text{s}$ . According to

Bhuyan and co-workers, the first two are due to the binding of methionines (Met80 or Met65) and histidines (His26 or His33) to the heme iron followed by the photodissociation of the CO ligand, and the slow one ( $\approx 770 \mu\text{s}$ ) is caused by the bimolecular recombination of CO and CytC. Any kinetic components slower than the CO recombination are not detected in the TA signal, which indicates that this signal is not a sensitive probe for global structural changes, such as protein folding. Overall, our experiments with TG and TA spectroscopy show the complementary nature of the two detection methods, and at this point one can conclude that components 1, 3, and 4 of Figure 2a are likely to be related to the folding process.

A quantitative analysis is given in the following discussion. In the TG experiment, the sample is excited by spatially modulated light intensity produced by the interference of two excitation light waves. The excited solute molecules can either return to the ground state by releasing the absorbed photon energy to the solvent (heating) or undergo photoreactions to produce new chemical species. The spatially modulated light therefore generates sinusoidal concentration modulations of 1) the heated or normal solvent (thermal grating) and 2) the depleted reactant and the new chemical species (species grating). These concentration modulations in turn lead to sinusoidal modulations in the refractive indices ( $\delta n$ ), which are finally monitored as a TG signal by the diffraction efficiency of a probe beam. As a result, the TG signal intensity  $I_{\text{TG}}$  is proportional to the square of the sum of the refractive index change due to 1) the thermal releasing process ( $\delta n_{\text{th}}(t)$ ) and 2) the sum of the refractive index changes of each chemical species ( $\sum \delta n_i(t)$ ) [Eq. (1)]:

$$I_{\text{TG}}(t) = \alpha \left[ \delta n_{\text{th}}(t) + \sum \delta n_i(t) \right]^2 \quad (1)$$

where  $\alpha$  is a constant. The TG signal intensity becomes weaker as the spatial modulation of the refractive index changes decays to zero. The decay of  $\delta n_{\text{th}}(t)$  occurs by the translational diffusion of the heat through the solvent. For  $\sum \delta n_i(t)$ , the decay can occur by either translational diffusion or further reactions of the chemical species (in this case, proteins).

In general, the refractive index change  $\delta n(t)$  due to translational diffusion is proportional to the Fourier transform of its concentration change,  $C(x,t)$ , given by solving a diffusion equation. For example, if  $D$  is time-independent and diffusion is the only process responsible for the decay of  $C(x,t)$ , then solving the diffusion equation gives the decay rate constant of  $Dq^2$ , that is,  $\delta n(t) = \delta n \exp(-Dq^2t)$ , where  $\delta n$  is the initial change in refractive index. For this reason,  $\delta n_{\text{th}}(t) = \delta n_{\text{th}} \exp(-D_{\text{th}}q^2t)$ , where  $\delta n_{\text{th}}$  is the initial refractive index change due to the thermal grating and  $D_{\text{th}}$  the thermal diffusivity of the solution. The CO photodissociation of unfolded CytC-CO depletes CytC-CO and generates unfolded CytC and CO within the instrument response time of the TG measurement. The decay of the refractive index change caused by the depleted CytC-CO can only occur by diffusion, and thus  $\delta n_{\text{CytC-CO}}(t) = \delta n_{\text{CytC-CO}} \exp(-D_{\text{CytC-CO}}q^2t)$ . If the photoproducts are formed within the excitation pulse width and do not involve further reactions, the

temporal progression of the TG signal can be expressed as follows [Eq. (2)]:

$$I_{\text{TG}}(t) = \alpha \left[ \delta n_{\text{th}} \exp(-D_{\text{th}}q^2t) + \sum_i \delta n_i \exp(-D_iq^2t) \right]^2 \quad (2)$$

where  $D_i$  is a diffusion coefficient of the chemical species. Initially it was attempted to fit the TG signal with this simple equation. It is straightforward to assign component 2 to the thermal grating signal. The  $Dq^2$  of the fast component 1 shows a constant value regardless of  $q^2$ , which means that its  $\delta n_i(t)$  is not due to a diffusion process but to fast protein dynamics. In other words,  $\delta n_i(t) = \delta n_i \exp(-k_i t)$  rather than  $\delta n_i \exp(-D_i q^2 t)$ . The fit quality is quite satisfactory in the early timescale (components 1 and 2). However, the  $Dq^2$  of subsequent signals (components 3 and 4) in the slower time region ( $\approx 10 \mu\text{s}$  to  $\approx 0.2 \text{ s}$ ) are not linearly proportional to  $q^2$  and the fit quality is not satisfactory. This finding indicates that Equation (2), which assumes that any new species, such as a folded protein, does not form by a folding process during diffusion, cannot properly explain the TG signal. This means that the folding processes occur in timescales similar to the diffusion process, and equations taking the folding kinetics into account more explicitly are necessary. This also suggests that component 3 results from the square of the sum of the refractive index changes due to species grating signals from not only unfolded proteins but also newly emerging folded proteins. Component 4 is also mainly due to the diffusion process of the proteins (both unfolded and folded). These assignments are confirmed in a quantitative analysis described below.

We compared our data with two folding models, namely, the two-state mechanism and the sequential mechanism. First, in the sequential mechanism, the protein structure continuously changes with time, and therefore, the  $D$  of the protein is time-dependent. The time dependence of  $D$  can be modeled by a single exponential function with a folding rate constant  $k_f$  [Eq. (3)]:

$$D(t) = D_U + (D_N - D_U)(1 - \exp(-k_f t)) \quad (3)$$

$D_U$  and  $D_N$  are the diffusion coefficients of unfolded (U) and folded (N) CytC, respectively. The time-dependent  $C(x,t)$  of the folded protein is governed by the following diffusion equation with time-dependent  $D(t)$  [Eq. (4)]:

$$\frac{\partial C(x,t)}{\partial t} = D(t) \frac{\partial^2 C(x,t)}{\partial x^2} \quad (4)$$

Solving the equation eventually provides the last term in the following equation for the TG signal [Eq. (5)]:

$$I_{\text{TG}}^{\text{sequential}} = \alpha \left[ \delta n_1 \exp(-k_1 t) - \delta n_{\text{th}} \exp(-D_{\text{th}}q^2t) + \delta n_{\text{CytC-CO}} \exp(-D_{\text{CytC-CO}}q^2t) + \delta n_N \exp \left[ -D_N q^2 t - \frac{(D_N - D_U)q^2}{k_f} (1 - \exp(-k_f t)) \right] \right]^2 \quad (5)$$

where  $\delta n_{\text{CytC-CO}}$  and  $\delta n_{\text{N}}$  are the initial refractive index changes due to CytC-CO and the folded CytC, respectively.

On the other hand, if the protein folds via the two-state mechanism with a protein folding rate ( $k_f$ ) as in the following pathway [Eq. (6)]:



the time dependence of each species is given by the following diffusion equations [Eqs. (7)]:

$$\begin{aligned} \frac{\partial \text{CytC-CO}(x,t)}{\partial t} &= D_{\text{CytC-CO}} \frac{\partial^2 \text{CytC-CO}(x,t)}{\partial x^2} \\ \frac{\partial U(x,t)}{\partial t} &= D_U \frac{\partial^2 U(x,t)}{\partial x^2} - k_f U(x,t) \\ \frac{\partial N(x,t)}{\partial t} &= D_N \frac{\partial^2 N(x,t)}{\partial x^2} - k_f N(x,t) \end{aligned} \quad (7)$$

Solving these equations by considering the similar molecular sizes of CytC-CO and CytC<sub>U</sub> ( $D_{\text{CytC-CO}} \approx D_U$ ) provides the last three terms in the TG signal for the two-state model as follows [Eq. (8)]:

$$\begin{aligned} I_{\text{TG}}^{\text{Two-State}} &= \alpha [\delta n_1 \exp(-k_1 t) - \delta n_{\text{th}} \exp(-D_{\text{th}} q^2 t) \\ &\quad + \delta n_{\text{CytC-CO}} \exp(-D_U q^2 t) + \delta n_U \exp\{-(D_U q^2 + k_f) t\} \\ &\quad + \frac{k_f}{(D_N - D_U) q^2 - k_f} \delta n_N [\exp\{-(D_U q^2 + k_f) t\} - \exp(-D_N q^2 t)]^2 \end{aligned} \quad (8)$$

Using these two mechanisms, we fit all TG signals by minimizing the discrepancy between the experiment and theory for all  $q$  values used in the measurement. The results of this global fitting analysis are depicted in Figure 3. The good agreement between theory and experiment for the two-state mechanism and about five times larger residuals for the sequential mechanism support the two-state mechanism for the folding reaction of CytC. The determined parameters are as follows;  $D_{\text{CytC-CO}} \approx D_U = 0.79 \pm 0.04 \times 10^{-10} \text{ m}^2 \text{ s}^{-1}$ ,  $D_N = 1.3 \pm 0.1 \times 10^{-10} \text{ m}^2 \text{ s}^{-1}$ ,  $k_1 = 1.4 \pm 0.1 \times 10^6 \text{ s}^{-1}$ , and  $k_f = 256 \pm 5 \text{ s}^{-1}$ .

Figure 3b shows all the decomposed individual exponential terms in Equation (8). Note that two grow-decay dynamics (components 3 and 4) are due to the square of the sum of the refractive index changes of various components in Equation (8). In particular, the grow-decay behavior of component 3 is dominated by the third and fourth terms of Equation (8), and another grow-decay dynamics of component 4 is dominated by the third and fifth terms of Equation (8).

The folding rate constant of  $256 \pm 5 \text{ s}^{-1}$  is slightly smaller than that ( $380 \text{ s}^{-1}$ ) determined by a stopped-flow experiment using two-syringe mixing.<sup>[21]</sup> In that experiment, the initial unfolded CytC solution prepared in 5 M Gd-HCl was diluted by mixing a folding buffer at pH 12.7, and the folding rate constants were measured for various final Gd-HCl concentrations, which were used to extrapolate and estimate the folding rate for zero denaturant concentration.<sup>[21]</sup> A much smaller constant of  $68 \text{ s}^{-1}$  was also reported from an experiment using a similar

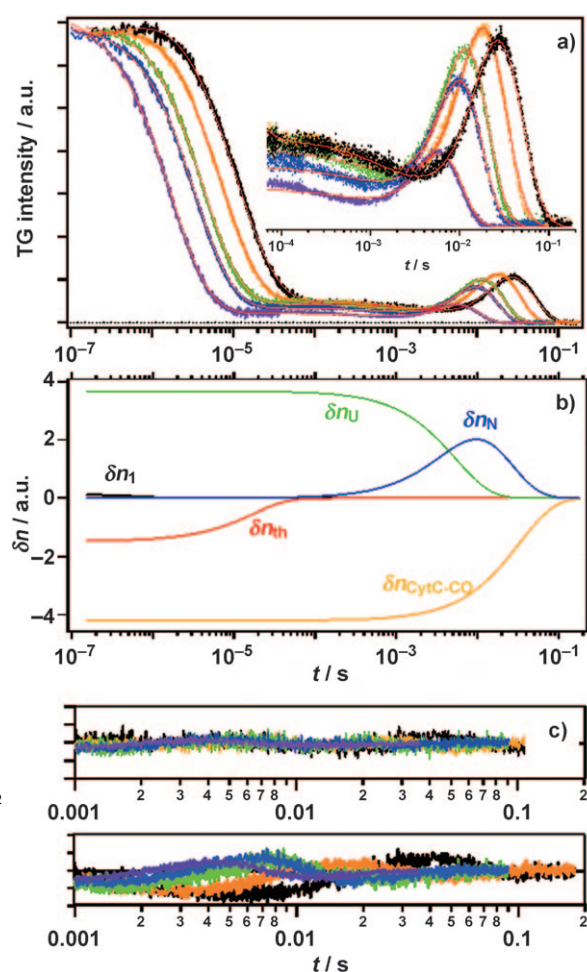


**Figure 3.** a) Global fitting results of the whole range of TG signals based on the two-state model. The theoretical fits obtained from the global fitting analysis are shown in red. Inset: expanded view of late time delays from 1 ms to 0.2 s. b) Schematic decomposition of the components of the TG signal according to the two-state model. The observed TG signal at  $q^2 = 0.39 \times 10^{12} \text{ m}^{-2}$  could be reproduced by taking the square of the sum of these components in Equation (8). c) Residuals of global fitting results for the two-state mechanism (top) and the sequential mechanism (bottom). It is evident that the observed TG signals are well reproduced by the two-state mechanism rather than the sequential mechanism.

stopped-flow method.<sup>[16]</sup> To determine the activation energy ( $E_a$ ) for the folding reaction of CytC, TG experiments were carried out at various temperatures (see Figure 4). Using the Arrhenius theory,  $E_a = -RT \ln(k_f/A)$ ;  $E_a$  and  $A$  were determined to be  $21.8 \pm 1.5 \text{ kcal mol}^{-1}$  and  $7.6 \pm 0.7 \times 10^{18} \text{ s}^{-1}$ , respectively. The folding energy barrier of  $21.8 \text{ kcal mol}^{-1}$  is larger than that reported in the literature ( $8.2 \text{ kcal mol}^{-1}$ ),<sup>[16]</sup> where the activation energy was estimated without any temperature-dependent measurements by using an estimated pre-exponential factor  $A$  from a literature value. If  $A$  determined from our TG measurements is used, a value similar to ours would result. Furthermore, our value is consistent with that estimated from the experimental results of Terazima and co-workers (see Figure 5 in ref. [17]).



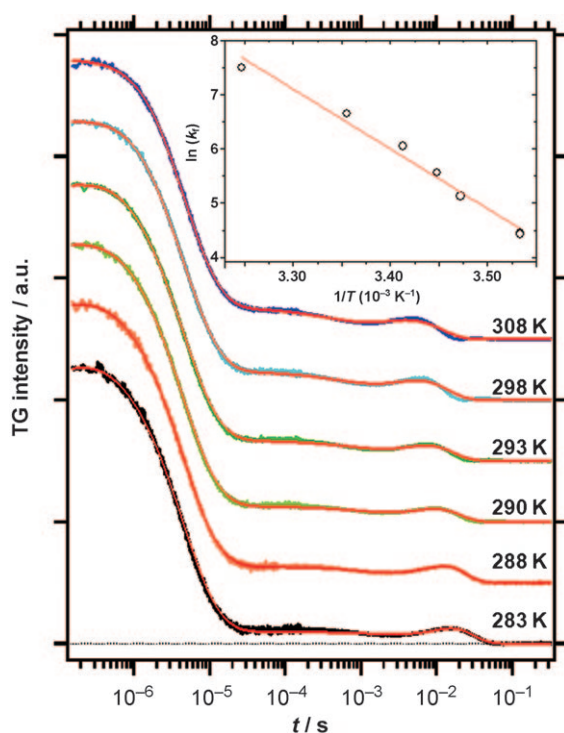


**Figure 4.** TG signals after photoexcitation of CytC-CO at  $q^2 = 1.96 \times 10^{12} \text{ m}^{-2}$  as a function of temperature. Inset: temperature dependence of the folding rate constants determined from the fitting of TG signals. The activation energy ( $E_a$ ) for the folding reaction of CytC is estimated to be  $21.8 \pm 1.5 \text{ kcal mol}^{-1}$ .

The folding time constant obtained in our TG measurement (3.9 ms) is considerably slower than the CO recombination time constant ( $\approx 770 \mu\text{s}$ ) from our TA experiment. Notably, the ratio of these two time constants determines the fraction of the folded proteins, and the current ratio (5:1) is not high enough to completely quench the folding pathway to the point where the TG signal due to folding is below the detection limit.

Now, we consider the origin of the component 1 ( $k_1$ ) observed in the time region of a few microseconds (see Figure 2b). The process at about 710 ns is probably due to the binding of several non-native ligands, such as His26, His33, and Met80 (or Met65), to the heme iron followed by the photodissociation of the CO ligand. Kumar et al. reported that the process observed at about  $0.33 \times 10^6 \text{ s}^{-1}$  ( $\approx 300 \text{ ns}$ ) in 1.5 mM CAPS containing 0.35 M Gd-HCl (pH 13) was due to the binding of methionines (Met80 or Met65) to the heme iron of the photoproduct ( $\text{Fe}^{\text{II}}\text{-Met}$ ).<sup>[21]</sup> Kligler et al. suggested that the  $\text{Fe}^{\text{II}}\text{-Met80}$  coordination after the photodissociation of the CO ligand took place with a rate constant of  $5 \times 10^5 \text{ s}^{-1}$  ( $2 \mu\text{s}$ ) in solution at pH 6.5 containing 4.6 M Gd-HCl.<sup>[5]</sup> Thus, in view of our Gd-HCl-free experimental conditions, the  $\approx 710 \text{ ns}$  kinetics may be attributed to the molecular volume change and the absorption change associated with the  $\text{Fe}^{\text{II}}\text{-Met}$  coordination. This is also consistent with our TA measurement (Figure 2d), in which the absorption change at 435 nm after photoexcitation of 200  $\mu\text{M}$  CytC-CO in a CAPS buffer solution (pH 13) has relaxa-

tion dynamics of  $\approx 0.9 \mu\text{s}$  due to the binding of methionines (Met80 or Met65). Since the absorption change of a protein due to  $\text{Fe}^{\text{II}}\text{-Met}$  coordination or the folding reaction at 780 nm is, however, too small, we attribute the main contribution of the  $\approx 710 \text{ ns}$  process to the molecular volume change induced by  $\text{Fe}^{\text{II}}\text{-Met}$  coordination. Because  $\delta n_{\text{th}}$  is generally negative, there would be no slowly rising component if  $\delta n_1$  were also negative. In other words, the presence of the slowly rising component indicates that  $\delta n_1$  is positive, thereby partly canceling the effect of  $\delta n_{\text{th}}$ . The positive  $\delta n_1$  decays over time, which indicates that the coordination of  $\text{Fe}^{\text{II}}\text{-Met}$  after photoexcitation of CytC results in the volume expansion. Indeed, it is well accepted that the unfolding of proteins leads to a volume decrease due to the exposure of charged/polar and nonpolar residues and the disruption of internal voids.<sup>[24–26]</sup> Thus, the  $\text{Fe}^{\text{II}}\text{-Met}$  coordination can lead to a small increase in volume. This volume expansion due to the coordination of  $\text{Fe}^{\text{II}}\text{-Met}$ , however, is substantially less than 1% of the specific volume of a protein.

On the other hand, the value of  $D_N$  determined from the global fitting ( $1.3 \pm 0.1 \times 10^{-10} \text{ m}^2 \text{ s}^{-1}$ ) is consistent with that of the native CytC reported previously ( $1.2\text{--}1.3 \times 10^{-10} \text{ m}^2 \text{ s}^{-1}$ ),<sup>[19,27]</sup> which indicates that the final state in our experiment is a fully folded native CytC. In contrast, the  $D_U$  value determined here ( $0.79 \pm 0.04 \times 10^{-10} \text{ m}^2 \text{ s}^{-1}$ ) is significantly larger than that of Gd-HCl-induced unfolded CytC at pH 7 ( $0.66 \times 10^{-10} \text{ m}^2 \text{ s}^{-1}$ ), determined by using a combination of the electron transfer of NADH and TG spectroscopy.<sup>[19]</sup> The difference between the values of  $D$  for two unfolded proteins may originate from the different denaturation conditions, that is, the structure of the unfolded protein induced by denaturant may be significantly different from that induced by CO ligation and high pH. Since it is generally known that a strong denaturant, such as Gd-HCl and urea, can induce the complete denaturation of a protein, the small value of  $D_U$  ( $0.66 \times 10^{-10} \text{ m}^2 \text{ s}^{-1}$ ) obtained at pH 7 with 4 M Gd-HCl represents the  $D$  of a completely denatured protein. Thus, the larger  $D_U$  obtained at pH 13 without any denaturant suggests that the conformation of the CO ligation- and pH-induced denatured CytC is not a completely random-coiled polypeptide but a partially folded one. By using a CD technique, Breslauer et al. reported that only 70–80% of the surface area of the base-induced unfolded CytC was exposed to the solvent, and the unfolded CytC at alkaline pH had a partially ordered structure compared to that observed in the presence of Gd-HCl or urea.<sup>[28]</sup> The larger  $D_U$  ( $0.79 \times 10^{-10} \text{ m}^2 \text{ s}^{-1}$ ) determined under our experimental conditions provides quantitative evidence that the denatured state of CytC in our study is significantly different from that induced by a denaturant.

In conclusion, we have investigated the optically triggered folding dynamics of CytC-CO by combining TG and TA spectroscopy, and have demonstrated the complementary nature of TG and TA. TG is sensitive to the global folding process that is not observed in TA, whereas CO recombination was visible only in TA. After photodissociation of the CO ligand from unfolded CytC-CO under strongly basic conditions, the TG signals show the methionine-binding process as well as the folding process, thus allowing us to provide the time constants for

both processes, which are summarized in Figure 5. A quantitative analysis of the TG signal supports two-state folding kinetics rather than multistate folding kinetics (sequential mecha-

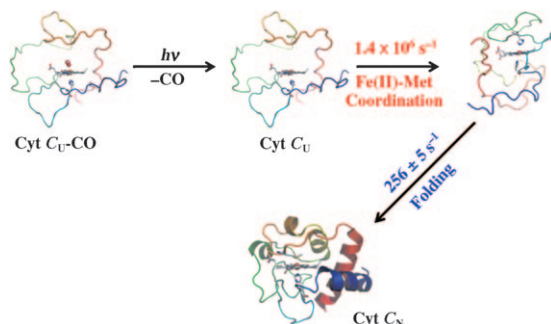


**Figure 5.** Schematic illustration of the folding reaction of CytC initiated by the photodissociation of the CO ligand determined by TG spectroscopy. Only the processes sensitive to TG are shown and others, such as CO recombination, are not shown.

nism). The activation energy ( $E_a$ ) for the folding reaction of CytC is also determined from temperature-dependent TG signals. In addition, the measured diffusion coefficient for the unfolded state provides strong evidence that the unfolded state at pH 13 is partially unfolded, unlike that in the presence of denaturant.

## Experimental Section

The experimental setup for the TG experiment was similar to those reported previously.<sup>[17,29]</sup> The second harmonic (532 nm) of an Nd:YAG laser (Brilliant B, pulse width 6–7 ns) was used as the excitation beam and a photodiode beam (780 nm, Thorlabs) as the probe beam. The diffracted probe beam (TG signal) was isolated from the excitation laser beam with a glass filter (Thorlabs FGL715S) and a pinhole. The isolated TG signal was detected by a photomultiplier tube (Hamamatsu R-928) and was fed into a digital oscilloscope (Tetronix TDS 3052B). The repetition rate of the photoexcitation was 2 Hz. The TG signal was averaged about 32 times to obtain a sufficient signal-to-noise ratio. The size of the excitation beam at the sample position was focused to be about 1 mm  $\phi$ . The laser-irradiated volume was small (typically ca.  $2 \times 10^{-3}$  cm<sup>3</sup>) compared with the total volume of the sample solution. The sample cell was kept inside a temperature-controlled holder (10–35 °C). Most experiments were conducted at room temperature.

CytC-CO was prepared by using the following method: Equine heart cytochrome c (CytC) was purchased from Sigma-Aldrich Co. The CytC solution in CAPS buffer (10 mM, pH 13) was placed in a rubber-topped airtight quartz cuvette (optical path length = 2 mm) and the concentration of CytC was adjusted to 1 mM. CytC was reduced by adding sodium dithionite (10 mM) to the CytC solution under a nitrogen atmosphere. CO gas was passed over the reduced sample for 30 min to fully convert CytC to the CO-bound CytC (CytC-CO). Finally, the sample cell was purged again with N<sub>2</sub> gas for several minutes. Even under this condition of dilute CO concentration (less than 0.02 mM), the fraction of the CO-unbound CytC was less than 1% of that of CytC-CO if the equilibrium association constant of about  $6 \times 10^5$  M<sup>-1</sup> was used.<sup>[21]</sup> In addition, the

photoreaction of the CO-unbound CytC did not affect the species grating signal. The sample solution was prepared just before measurement.

The value of  $q$  in the TG measurement was determined from the decay rate of the thermal grating signal of a reference sample, bromocresol purple, which gave rise to only the thermal grating signal due to nonradiative transition within the pulse width of the excitation laser. Since in the high  $q^2$  range ( $> 1 \times 10^{13}$  m<sup>-2</sup>) the diffusion process of a protein takes place on the order of submilliseconds and this timescale is much faster than the folding rate, it is very difficult to trace the protein folding dynamics. Thus, all TG measurements were carried out with a small  $q^2$  range ( $\leq 2.5 \times 10^{12}$  m<sup>-2</sup>) where the folding rate of a protein is on the same order of time-scale as the diffusion rate, and thus the TG signal associated with the diffusion process is more sensitive to the folding process.

TA spectroscopy was performed on 200  $\mu$ M CytC-CO in a CAPS buffer solution (pH 13) by using the second harmonic (532 nm) of an Nd:YAG laser (Brilliant B, pulse width 6–7 ns) as the excitation source and a 250-W Xe lamp as the probing light source. The probing light was oriented perpendicular to the excitation laser beam, passed through a grating monochromator, and detected with a photomultiplier (Hamamatsu R-928) and a digital oscilloscope (Tetronix TDS 3052B).

## Acknowledgements

This work was supported by Creative Research Initiatives (Center for Time-Resolved Diffraction) of MOST/KOSEF and by the MEST/KOSEF (R11-2005-00000-0).

**Keywords:** cytochrome c • diffusion coefficients • photochemistry • protein folding • transient grating spectroscopy

- [1] W. Qiu, L. Zhang, Y. T. Kao, W. Lu, T. Li, J. Kim, G. M. Sollenberger, L. Wang, D. Zhong, *J. Phys. Chem. B* **2005**, *109*, 16901.
- [2] C. Travaglini-Allocatelli, S. Gianni, M. Brunori, *Trends Biochem. Sci.* **2004**, *29*, 535.
- [3] K. Noyelle, M. Joniau, H. Van Dael, *J. Mol. Biol.* **2001**, *308*, 807.
- [4] S. Akiyama, S. Takahashi, K. Ishimori, I. Morishima, *Nat. Struct. Biol.* **2000**, *7*, 514.
- [5] E. Chen, M. J. Wood, A. L. Fink, D. S. Klinger, *Biochemistry* **1998**, *37*, 5589.
- [6] X. Xie, J. D. Simon, *Biochemistry* **1991**, *30*, 3682.
- [7] Y. Goto, A. L. Fink, *J. Mol. Biol.* **1990**, *214*, 803.
- [8] T. E. Creighton, *Biochem. J.* **1990**, *270*, 1.
- [9] W. A. Eaton, P. A. Thompson, C. K. Chan, S. J. Hage, J. Hofrichter, *Structure* **1996**, *4*, 1133.
- [10] Z. D. Su, M. T. Arooz, H. M. Chen, C. J. Gross, T. Y. Tsong, *Proc. Natl. Acad. Sci. USA* **1996**, *93*, 2539.
- [11] R. Kumar, A. K. Bhuyan, *Biochemistry* **2005**, *44*, 3024.
- [12] R. Gilmanshin, S. Williams, R. H. Callender, W. H. Woodruff, R. B. Dyer, *Proc. Natl. Acad. Sci. USA* **1997**, *94*, 3709.
- [13] X. L. Xie, J. D. Simon, *Biochim. Biophys. Acta* **1991**, *1057*, 131.
- [14] Y. Oori, *Biochemistry* **1993**, *32*, 11910.
- [15] C. M. Jones, E. R. Henry, Y. Hu, C. K. Chan, S. D. Luck, A. Bhuyan, H. Roder, J. Hofrichter, W. A. Eaton, *Proc. Natl. Acad. Sci. USA* **1993**, *90*, 11860.
- [16] A. K. Bhuyan, D. K. Rao, N. P. Prabhu, *Biochemistry* **2005**, *44*, 3034.
- [17] T. Nada, M. Terazima, *Biophys. J.* **2003**, *85*, 1876.
- [18] S. Nishida, T. Nada, M. Terazima, *Biophys. J.* **2004**, *87*, 2663.
- [19] S. Nishida, T. Nada, M. Terazima, *Biophys. J.* **2005**, *89*, 2004.
- [20] M. Terazima, *Phys. Chem. Chem. Phys.* **2006**, *8*, 545.
- [21] R. Kumar, N. P. Prabhu, A. K. Bhuyan, *Biochemistry* **2005**, *44*, 9359.

- [22] O. Zhang, J. D. Forman-Kay, *Biochemistry* **1997**, *36*, 3959.  
[23] T. M. Logan, Y. Theriault, S. W. Fesik, *J. Mol. Biol.* **1994**, *236*, 637.  
[24] T. V. Chalikian, K. J. Breslauer, *Biopolymers* **1996**, *39*, 619.  
[25] M. Gross, R. Jaenicke, *Eur. J. Biochem.* **1994**, *221*, 617.  
[26] V. V. Mozhaev, K. Heremans, J. Frank, P. Masson, C. Balny, *Proteins* **1996**, *24*, 81.  
[27] C. B. Fuh, S. Levin, J. C. Giddings, *Anal. Biochem.* **1993**, *208*, 80.  
[28] T. V. Chalikian, V. S. Gindikin, K. J. Breslauer, *FASEB J.* **1996**, *10*, 164.  
[29] N. Baden, M. Terazima, *J. Phys. Chem. B* **2006**, *110*, 15 548.

---

Received: May 10, 2008

Revised: August 21, 2008

Published online on October 20, 2008

---